Estimation of State of Charge, Unknown Nonlinearities, and State of Health of a Lithium-Ion Battery Based on a Comprehensive Unobservable Model

Mehdi Gholizadeh and Farzad R. Salmasi, *Senior Member, IEEE*

***Abstract*—This paper considers the estimation of the state of charge and state of health for lithium-ion batteries, while an inclusive model is taken into account. The model includes two RC subnetworks, which represent the fast and slow transient responses of the terminal voltage. Nevertheless, the linear part of the model is unobservable. On the other hand, the nonlinear behavior of the open-circuit voltage versus state of charge is also included in the model. The proposed observer tackles the aforementioned problems to attain a reliable estimation of the state of charge. Moreover, as opposed to the methods in which the nonlinearities or uncertainties in the model are disregarded or those terms are discarded using a conventional sliding-mode observer, an analytical method is considered to estimate the additive nonlinear or uncertainty term in the model. This approach leads to a very accurate model of the battery to be used in a battery management system. Moreover, an online parameter estimation method is proposed to estimate the battery's state of health. The proposed scheme benefits from an adaptive rule for the online estimation of the series resistance in the lithium-ion battery based on the accurately identified model. Experimental tests certify the performance and feasibility of the proposed schemes.**

***Index Terms*—Adaptive observer, estimation, lithium-ion battery, sliding motion, state of charge, state of health (SoH).**

I. Introduction

LITHIUM batteries have been used recently in many applications such as portable power products and hybrid electric vehicles. They play a significant role in powering these technologies. To obtain the usable charge of the battery, to manage it to its optimal potential, and to extend the lifetime of the battery, it is required to monitor the available charge or state of charge (SoC) of the battery more accurately. The SoC, by definition, is the ratio of the available capacity to its maximum capacity when the cell is completely charged [1]. There have been more than a dozen of schemes presented by researchers in recent years to improve the SoC estimation. Coulomb counting or ampere-hour counting is the most commonly used method for SoC estimation in which the time integral of the battery current is considered as a direct SoC indication [2] as follows:

$$SoC(t) = SoC(t_0) - \int_{t_0}^{t} \frac{\eta I}{3600 C_n} d\tau \tag{1}$$

where $SoC(t_0)$ is the initial value of the SoC, C_n stands for the nominal capacity of the battery (in ampere-hours), I is the instantaneous current (positive for discharge and negative for charge), and η represents the Coulomb coefficient. However, this method accumulates errors in measurements and may lead to large SoC errors in real-world applications. An improved ampere-hour counting method is reported in which the open-circuit voltage (OCV) is taken into account. The measured OCV is used for the periodic correction of the SoC estimated by ampere-hour counting [3]. However, OCV can only be measured after a long rest of the battery. Hence, this strategy is not desirable in practice. In [4], the electromotive force (EMF) voltage of the battery is used to predict SoC. The EMF is approximated based on the impedance, load current, and terminal voltage of lead–acid and lithium-ion batteries.

The Kalman filter is inherently a recursive algorithm for the estimation of internal states of a dynamic system. It has been widely used for estimating the OCV or other parameters of the battery which have direct relation with the SoC (e.g., see [5]–[7]). To take the nonlinear behavior of OCV versus SoC into account, a nonlinear extension of this filter, known as the extended Kalman filter (EKF), is considered. EKF is another popular statistical tool to extract internal battery parameters such as SoC [8]–[10]. Furthermore, EKF is deployed by Kim and Cho to estimate both the SoC and state of health (SoH) of lithium-ion batteries, as reported in [11] and [12]. It should be noted that assumptions on certain statistical properties, along with the local linearization of the state equations, are the drawbacks of this renowned filter. Improved versions of EKF such as the sigma-point EKF [13] and adaptive EKF [14] are also reported for battery applications.

Adaptive and robust observers are also utilized for state estimation in batteries. An H_∞ observer is designed to estimate SoC based on a linear battery model in [15]. Li *et al.* used a class of piecewise linear systems as the lithium-ion battery model and then proposed an adaptive observer based on the model estimate SoC [16]. Artificial neural networks

Manuscript received October 20, 2012; revised January 15, 2013 and February 28, 2013; accepted March 26, 2013. Date of publication April 24, 2013; date of current version August 23, 2013.

The authors are with the Faculty of Engineering, School of Electrical and Computer Engineering, University of Tehran, Tehran 14395, Iran (e-mail: m.gholizadeh@ut.ac.ir; farzad_rs@ieee.org).

Color versions of one or more of the figures in this paper are available online at http://ieeexplore.ieee.org.

Digital Object Identifier 10.1109/TIE.2013.2259779

(ANNs) and fuzzy logic identifiers (FLIs) are other adaptive or intelligent alternatives for estimating SoC. In [17], fuzzy logic models were used by Sing *et al.* for SoC estimation and available capacity approximation based on measuring the electrochemical impedance spectroscopy of nickel/metal batteries. Aside from fuzzy logic, ANNs have gained much popularity for estimation and prediction, specifically for direct SoC estimation [18]–[21]. In [22], a neuro-fuzzy identifier known as locally linear model tree network is developed for SoC approximation. Although ANNs take the nonlinearities of the battery model into account, they suffer from the training process and the dependence to large training data sets. ANNs and FLIs are also reported as SoH estimators [23], [24]. Recently, the impulse response of a lithium battery is used for online SoC estimation [25].

In the presence of modeling errors and uncertainties, sliding-mode observers (SMOs) have been used as a reliable and robust tool for SoC or SoH estimation [26]. Kim proposed a SMO based on a simple RC model for SoC estimation, which was robust to the modeling uncertainties [27]. He extended his approach to evaluate the lithium battery SoH by the adaptive estimation of the series capacitance and resistance as the indicators of battery SoH, as reported in [28]. Recently, Einhorn *et al.* used the measured SoC at two states and the transferred charge between those states to estimate the cell capacity for lithium-ion batteries [29].

In this paper, new schemes for estimating the SoC and SoH of lithium-ion batteries are proposed, while an inclusive model is taken into account. The model encloses two RC networks, a series resistor, and a nonlinear voltage source with a parallel RC circuit. Nevertheless, designating the terminal and RC subnetwork voltages, along with the SoC, as the model dynamical states, the system state equation is linearly unobservable. This problem is a setback to directly develop an observer for the system. On the other hand, the nonlinear behavior of the OCV versus SoC is also encompassed by the model. The proposed SMO tackles the aforementioned problems. Moreover, unlike the methods that disregard the nonlinearities or uncertainties in the model or dump those terms using a conventional SMO, an analytical method is considered to estimate the additive nonlinear or uncertainty term in the model. This leads to a very accurate model of the battery for control and management purposes. Finally, an online parameter estimation method is proposed to estimate the SoH of the battery. This method uses an adaptive rule to estimate the series resistance of the battery based the accurately identified battery model. Experiments are performed for the verification of the proposed methods. Contributions of the scheme can be summarized as follows:

1) SoC estimation based on an unobservable but detectable nonlinear comprehensive model for lithium batteries;
2) direct estimation of battery model nonlinearities and uncertainties to derive an inclusive model of lithium batteries;
3) SoH estimation for the lithium battery based on the derived inclusive model with an identified additive term which represents nonlinearities and uncertainties.

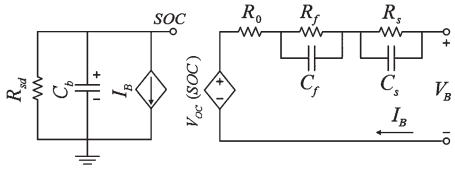

Fig. 1. Equivalent circuit model of the lithium-ion battery.

II. Comprehensive Battery Model

Due to the variety of applications for electrochemical batteries, the reported battery models cover a wide spectrum. Nevertheless, they can be classified into electrochemical, mathematical, intelligent, and electrical models. Electrical models are more apt to be used for estimation and control purposes. In the proposed scheme, an inclusive verified electrical battery model proposed by Chen and Rincon-Mora in [30] is adopted, as shown in Fig. 1. This electrical model mimics the precise dynamic behavior of the lithium-ion battery.

In this model, the nonlinear mapping from the battery's state of charge to the OCV is represented by a controlled voltage source, V_{oc}. Furthermore, an instantaneous terminal voltage variation due to the load current I_B is given by inserting a series resistance denoted by R_0. Nevertheless, for a step load current change, the terminal voltage response is far from an ideal step waveform, as it shows short and long time constant dynamics. These dynamics are modeled by two series RC networks, denoted by (R_f, C_f) and (R_s, C_s), respectively. The whole-charge capacitor is denoted by C_b, and the self-discharge energy loss due to long time storage is represented by R_{sd}. Owing to the slow variation of the no-load battery's usable capacity, the self-discharge resistance may be taken out of the picture, but in order to be more precise, it is included in the model in our scheme.

The dynamics of the voltages across the capacitors, V_f and V_s, are given by

$$\begin{aligned} \dot{V}_f &= -\frac{1}{R_f C_f} V_f + \frac{1}{C_f} I_B \\ \dot{V}_s &= -\frac{1}{R_s C_s} V_s + \frac{1}{C_s} I_B \end{aligned} \tag{2}$$

where I_B is the battery terminal current. The voltage across the whole-charge capacitor is V_{SoC}, and its dynamic is given by

$$\dot{V}_{SoC} = -\frac{1}{R_{sd} C_b} V_{SoC} - \frac{1}{C_b} I_B. \tag{3}$$

The battery terminal voltage can be expressed as

$$V_B = V_{oc} - R_0 I_B - V_f - V_s. \tag{4}$$

$V_{oc}(SoC)$ has an almost linear behavior in the region between 10% and 100% SoC and exponentially drops while the SoC is approximately below 10%. Therefore, the OCV is related to the SoC as follows:

$$V_{oc} = \alpha V_{SoC} + g(V_{SoC}) \tag{5}$$

where $g(V_{SoC})$ stands for the nonlinear part of the OCV. Given the fact that the rate of change of the terminal current is

negligible in comparison with other time constants in a sampling period, the time derivative of the terminal voltage is determined to be

$$\dot{V}_B = \frac{\partial V_{oc}}{\partial V_{SoC}}\dot{V}_{SoC} - \dot{V}_f - \dot{V}_s$$
$$\frac{\partial V_{oc}}{\partial V_{SoC}} = \alpha + \dot{g}(V_{SoC}). \tag{6}$$

From (3), (4), and (6), the dynamic of the terminal voltage is determined to be

$$\dot{V}_B = \left(-\frac{\alpha}{R_{sd}C_b} + \frac{\alpha}{R_sC_s}\right)V_{SoC} + \left(\frac{1}{R_fC_f} - \frac{1}{R_sC_s}\right)V_f - \frac{1}{R_sC_s}V_B - \left(\frac{R_0}{R_sC_s} + \frac{\alpha}{C_b} + \frac{1}{C_f} + \frac{1}{C_s}\right)I_B + \Phi(V_{SoC}, I_B) \tag{7}$$

where $\Phi(V_{SoC}, I_B)$ stands for the nonlinearities in the terminal voltage dynamic. Moreover, the modeling uncertainties are considered to be embedded into this term.

Defining $\xi[V_{SoC}V_fV_SV_B]^T$ as the state vector and denoting the battery current and terminal voltage as the system input and output, respectively, the state and output equations of the battery based on the adopted model are given by

$$\dot{\xi} = A\xi + BI_B + D\Phi \quad V_B = C\xi \tag{8}$$

where

$$A = \begin{bmatrix} -\frac{1}{R_{sd}C_b} & 0 & 0 & 0 \\ 0 & -\frac{1}{R_fC_f} & 0 & 0 \\ 0 & 0 & -\frac{1}{R_sC_s} & 0 \\ -\frac{\alpha}{R_{sd}C_b}+\frac{\alpha}{R_sC_s} & \frac{1}{R_fC_f}-\frac{1}{R_sC_s} & 0 & -\frac{1}{R_sC_s} \end{bmatrix}$$
$$B = [\,b_1 \quad b_2 \quad b_3 \quad b_4\,]^T, C = D^T = [\,0 \quad 0 \quad 0 \quad 1\,]$$
$$b_1 = -\frac{1}{C_b}, b_2 = -\frac{1}{C_f}, b_3 = \frac{1}{C_s},$$
$$b_4 = -\frac{R_o}{R_sC_s} - \frac{\alpha}{C_b} - \frac{1}{C_f} - \frac{1}{C_s}.$$

The observability matrix of the linear system is given by $[C \;\; CA \;\; CA^2 \;\; CA^3]^T$. It turns out that one column in this matrix is zero. Therefore, the battery model is unobservable. This problem is a setback to design any observer to estimate the state vector ξ. However, since the A-matrix is stable, the battery model is detectable. It should be noted that $\Phi[V_{SoC}, I_B]$ is bounded with respect to the battery current. Therefore, there exists $\varphi(I_B)$ such that

$$|\Phi(V_{SoC}, I_B)| \leq \vartheta(I_B). \tag{9}$$

III. Observer Design For SoC Estimation

In this section, a sliding-mode-type observer is designed for the robust estimation of the states of the lithium-ion battery based on the unobservable model in (8). Later, using the designed observer, the nonlinear part of the battery model, $\Phi[V_{SoC}, I_B]$ is estimated directly to attain an inclusively identified battery model. The proposed observer is as follows:

$$\dot{\hat{\xi}} = A\hat{\xi} + BI_B + Me_{V_B} + \mu D\rho(e_{V_B}) \quad \hat{V}_B = C\hat{\xi}. \tag{10}$$

It should be noted that $e_{V_B} = V_B - \hat{V}_B$. The observer correction function is chosen as follows:

$$\rho(e_{V_B}) = \frac{e_{V_B}(t)}{|e_{V_B}(t)| + \gamma(t)} \tag{11}$$

where $\gamma(t) : \mathbb{R}^+ \to \mathbb{R}^+$ is a continuous function such that $\dot{\gamma} < -c\gamma(t)$ and c is a positive scalar. Observer gain matrix M could be determined by pole assignment, but the pair (A, B) is unobservable. Thus, it hinders us to design the observer directly. To overcome this setback, the system dynamic is decomposed into observable and unobservable modes. Therefore, the observable modes of the system can be arbitrarily placed. The decomposed system equations are given by

$$\begin{bmatrix} \dot{\xi}_o \\ \dot{\xi}_u \end{bmatrix} = \begin{bmatrix} A_o & 0 \\ 0 & A_u \end{bmatrix}\begin{bmatrix} \xi_o \\ \xi_u \end{bmatrix}\begin{bmatrix} B_o \\ B_u \end{bmatrix} I_B + \overline{D}\Phi(V_{SoC}, I_B)$$
$$V_B = \overline{C}\begin{bmatrix} \xi_o \\ \xi_u \end{bmatrix} \tag{12}$$

where ξ_u and ξ_o denote the observable and unobservable modes, respectively. Moreover

$$A_o = \begin{bmatrix} -\frac{1}{R_{sd}C_b} & 0 & 0 \\ 0 & -\frac{1}{R_fC_f} & 0 \\ -\frac{\alpha}{R_{sd}C_b}+\frac{\alpha}{R_sC_s} & \frac{1}{R_fC_f}-\frac{1}{R_sC_s} & -\frac{1}{R_sC_s} \end{bmatrix}$$
$$A_u = -\frac{1}{R_sC_s}, B_0 = [\,b_1 \quad b_2 \quad b_4\,]^T, B_u = -\frac{1}{C_s}$$
$$\overline{D} = [\,D_0^T \quad 0\,]^T, \overline{C} = [\,C_o \quad 0\,]$$
$$C_o = D_o^T = [\,0 \quad 0 \quad 1\,]. \tag{13}$$

Since the unobservable subsystem A_u is stable, the system is detectable. Also, the observer gain is considered to be $M = [M_o \quad 0]^T$. Therefore, the observer dynamics are decomposed as follows:

$$\begin{bmatrix} \dot{\hat{\xi}}_o \\ \dot{\hat{\xi}}_u \end{bmatrix} = \begin{bmatrix} A_o & 0 \\ 0 & A_u \end{bmatrix}\begin{bmatrix} \hat{\xi} \\ \hat{\xi}_u \end{bmatrix} + \begin{bmatrix} B_o \\ B_u \end{bmatrix} I_B \begin{bmatrix} M_o \\ 0 \end{bmatrix} e_{V_B} + \mu\overline{D}\rho(e_{V_B})$$
$$\hat{V}_B = \overline{C}\begin{bmatrix} \xi_o \\ \hat{\xi}_u \end{bmatrix}. \tag{14}$$

For the observable subsystem, M_o is obtained arbitrarily using pole placement. Therefore, for a given $Q_o > 0$, there exists a symmetric $P_o > 0$ such that

$$P_o(A_o - M_oC_o) + (A_o - M_oC_o)^T P_o = -Q_o. \tag{15}$$

Subtracting (14) from (12), the state estimation error system is obtained as follows:

$$\dot{e} = \begin{bmatrix} \dot{e}_o \\ \dot{e}_u \end{bmatrix} = \begin{bmatrix} A_o - M_oC_o & 0 \\ 0 & A_u \end{bmatrix}\begin{bmatrix} e_o \\ e_u \end{bmatrix} + \overline{D}\Phi(V_{SoC}, I_B) - \mu\overline{D}\rho(e_{V_B})$$
$$e_{V_B} = \overline{C}e = \overline{C}\begin{bmatrix} e_o \\ e_u \end{bmatrix}. \tag{16}$$

A conventional Lyapunov function for the error system is given by

$$V(e) = e^{\tau} P e. \tag{17}$$

The $P\_$ matrix is chosen to be $\mathrm{diag}(P_0, 1)$. Moreover, it is assumed that, for some $F > 0$, $F\bar{C} = \bar{D}^T P$. This is a common assumption in the sliding-mode literature (e.g., see [31]).

The determination of the derivative of the above function along the error trajectory in (16) yields

$$\begin{aligned}\dot{V}(e) &= \dot{e}Pe + e^T P\dot{e} = \begin{bmatrix}\dot{e}_o \\ \dot{e}_u\end{bmatrix}^T P \begin{bmatrix}e_o \\ e_u\end{bmatrix}^T P \begin{bmatrix}\dot{e}_o \\ \dot{e}_u\end{bmatrix} \\ &= -e_o^T Q_o e_o + 2e_u^T A_u e_u + 2\overline{D}^T Pe\,(\Phi - \mu\rho(e_{V_B})) \\ &= -e_o^T Q_o e_o - \frac{2}{R_s C_s}|e_u|^2 \\ &\quad + 2Fe_{V_B}\left(\Phi - \mu\frac{e_{V_B}}{|e_{V_B}| + \gamma(t)}\right).\end{aligned} \tag{18}$$

On the other hand, we have

$$\frac{e_{V_B}^2}{|e_{V_B}| + \gamma(t)} = |e_{V_B}| - \gamma(t) + \frac{\gamma^2}{|e_{V_B}| + \gamma} = |e_{V_B}| - \delta(t). \tag{19}$$

Since $\gamma(t)$ is positive for every t, then

$$\delta(t) = \gamma(t) - \frac{\gamma^2}{|e_{V_B}| + \gamma} > 0. \tag{20}$$

Consequently, it leads to the following inequality:

$$\begin{aligned}\dot{V}(e) \le -\lambda_{\min}(Q_0)\|e_o\|^2 - \frac{2}{R_s C_s}|e_u|^2 + 2F\mu\delta(t) \\ +2F\left(e_{V_B}\Phi - \mu|e_{V_B}|\right).\end{aligned} \tag{21}$$

Since $\dot{\gamma}(t) < -c\gamma(t)$, $\delta(t)$ asymptotically converges to zero. Therefore, if μ is chosen such that

$$\mu > \vartheta(I_B) > |\Phi(V_{SoC}, I_B)| \tag{22}$$

then $\dot{V}(e) < 0$, and consequently, the asymptotic stability of the error system is ensured. Thus, the estimated SoC voltage converges to the real value.

IV. Estimation of Nonlinearities

The battery model in (8) is not thoroughly identified if the nonlinear term $\Phi(V_{SoC}, I_B)$ is not reconstructed. The estimation of SoC based on the SMO relies only on an upper bound of this term. Nevertheless, in order to simulate the battery transient responses and design charge controllers and battery management systems, the reconstruction of the nonlinear behavior of the battery is unavoidable. Although nonlinear approximators such as neural networks or fuzzy identifiers may be utilized for this purpose, they require a large number of training data sets. In the new scheme, we extended the results from the last section to analytically estimate the nonlinear term.

In the previous section, the state estimation error system has been obtained by decomposing the system to observable and unobservable modes, as it appears in (12).

Defining $\bar{A}_o = A_o - M_o C_o$, then, the dynamic of the observable error subsystem is given by

$$\begin{aligned}\dot{e}_o &= \bar{A}_o e_o + D_o\Phi(V_{SoC}, I_B) - \mu D_o\rho(e_{V_B}) \\ e_{V_B} &= C_o e_o = [\,0 \quad 0 \quad 1\,]\, e_o.\end{aligned} \tag{23}$$

Decomposing e_o and matrix $\bar{A}_o$ as follows:

$$e_o = \begin{bmatrix}e_{o1} \\ e_{V_B}\end{bmatrix}, \bar{A}_o = \begin{bmatrix}\bar{A}_{o11} & \bar{A}_{o12} \\ \bar{A}_{o21} & -\frac{1}{R_s C_s}\end{bmatrix} \tag{24}$$

results in

$$\begin{aligned}\dot{e}_{o1} &= \bar{A}_{o11}e_{o1} + \bar{A}_{o12}e_{V_B} \\ \dot{e}_{V_B} &= \bar{A}_{021}e_{o1} - \frac{1}{R_s C_s}e_{V_B} + \Phi(V_{SoC}, I_B) - \mu\rho(e_{V_B}).\end{aligned} \tag{25}$$

For this end, it is shown that, with the proposed observer, the error vector asymptotically converges to zero, i.e., $\lim_{t\to\infty} e_o(t) = 0$. Consequently, $e_{o1}(t)$ is bounded such that $\|\bar{A}_{21}e_{o1}\| \le \sigma$. In order to show that a sliding motion takes place in finite time, i.e., $e_{V_B} = \dot{e}_{V_B} = 0$, the reachability condition should be verified. For this purpose, we have

$$e_{V_B}\dot{e}_{V_B} = e_{V_B}\bar{A}_{21}e_{o1} - \frac{1}{R_s C_s}e_{V_B}^2 - e_{V_B}\left(\mu\rho(e_{V_B}) - \phi\right) \tag{26}$$

with $\mu > \varphi(I_B) > \Phi(V_{SoC}, I_B)$ and $\|\bar{A}_{21}e_{o1}\| \le \sigma$, and it yields to

$$\begin{aligned}e_{V_B}\dot{e}_{V_B} \le \sigma|e_{V_B}|\frac{1}{R_s C_s}e_{V_B}^2 - |e_{V_B}|\left(\mu - \gamma(I_B)\right) \\ +e_{V_B}\delta(t) \le -\xi|e_{V_B}| + e_{V_B}\delta(t)\end{aligned} \tag{27}$$

in which $\xi = (\mu - \gamma(I_B) - \sigma)$. Therefore, if

$$\mu > \gamma(I_B) + \sigma \tag{28}$$

and considering the fact that $\delta(t)$ asymptotically converges to zero, then we conclude that the sliding motion maintains thereafter. Now, from (25), during the sliding motion, we have

$$\Phi(V_{SoC}, I_B) = \mu\rho(e_{V_B}) - \bar{A}_{21}e_{o1} \tag{29}$$

where ρ_{eq} is known as the equivalent output injection signal [32]. Let us introduce the estimated nonlinear term as follows:

$$\widehat{\Phi}(V_{SoC}, I_B) = \mu\rho(e_{V_B}) = \mu\frac{e_{V_B}(t)}{|e_{V_B}(t)| + \gamma(t)}. \tag{30}$$

Then, we have

$$|\Phi - \widehat{\Phi}| = \left|\mu\rho_{eq} - \bar{A}_{21}e_{o1} - \mu\rho\right| \le \left\|\bar{A}_{21}\right\|\|e_{o1}\| + \mu|\rho_{eq} - \rho|. \tag{31}$$

Since $\lim_{t\to\infty}(\rho_{eq} - \rho) = 0$ and e_{o1} tends to zero, it follows that

$$\lim_{t\to\infty}|\Phi - \widehat{\Phi}| = 0. \tag{32}$$

V. SoH Estimation Based on Adaptive Observer

There are several definitions for SoH such as the battery cell's capability of storing energy and preserving charge for long periods [23] or the ratio of the amount of charge that can be drawn from a new battery to the aged battery [24]. The battery cranking ability has been used as a token for battery SoH approximation by Cugnet *et al.* [33].

Evaluating the battery SoH, a battery management system may conclude about the battery's end of life (EoF) and signals for the replacement or restrict the number of cycles [5]. The increase and decrease of series resistance and capacitance, respectively, are reported as the indications of reduced SoH by Kim in [27]. In [5], the 60% decrease of battery maximum power compared to its initial value is reported to be an indication of the battery's EoF. Thus, battery EoF is detected once the series resistance of the battery reaches to 160% of its initial value at the same condition of temperature and SoC, i.e., [34]

$$SoH = \frac{R_{0,EoF} - R_0}{R_{0,EoF} - R_{0,\text{new}}} \times 100\% \tag{33}$$

where R_0, $R_{0,EoF}$, and $R_{0,\text{new}}$ denote the current, the EoF, and the new battery series resistance.

In the following, an adaptive scheme is developed to estimate the series resistance as an indicator of SoH based on the inclusive battery model in (8) and the results of the last sections. The proposed SoH estimator has the following structure:

$$\dot{\bar{\xi}} = A\bar{\xi} + \overline{B}I_B + D\widehat{\Phi}(V_{SoC}, I_B). \tag{34}$$

It should be noted that R_0 only appears in the B-matrix. Therefore, in the above observer equation, an estimated B-matrix, i.e., $\bar{B}$, is substituted. The estimation error dynamics is given by

$$\dot{\epsilon} = \dot{\xi} - \dot{\bar{\xi}} = A\epsilon + (B - \bar{B})I_B + D(\Phi - \widehat{\Phi}). \tag{35}$$

Moreover

$$B - \bar{B} = -\frac{\tilde{R}_0}{R_s C_s} D \tag{36}$$

where $\tilde{R}_0 = R_0 - \hat{R}_0$. The estimated resistance is denoted by $\hat{R}_0$. Based on the above dynamic, a simple adaptive observer is designed to estimate the series resistance. The following Lyapunov function:

$$\bar{V}(\epsilon) = -\frac{1}{2}\epsilon^T M\epsilon + \frac{1}{2\tau}\tilde{R}_0^2, \quad M > 0 \tag{37}$$

yields to

$$\dot{\bar{V}}(\epsilon) = -\frac{1}{2}\epsilon^T N\epsilon + (B-\bar{B})^T M\epsilon\, I_B - \frac{1}{\tau}\tilde{R}_0\dot{\hat{R}}_0 + \epsilon^T MD(\Phi - \widehat{\Phi}). \tag{38}$$

With the following adaptation rule:

$$\dot{\hat{R}}_0 = \tau DM\epsilon \tag{39}$$

we have

$$\dot{\bar{V}}(\epsilon) = -\frac{1}{2}\epsilon^T N\epsilon + \epsilon^T MD(\Phi - \widehat{\Phi}). \tag{40}$$

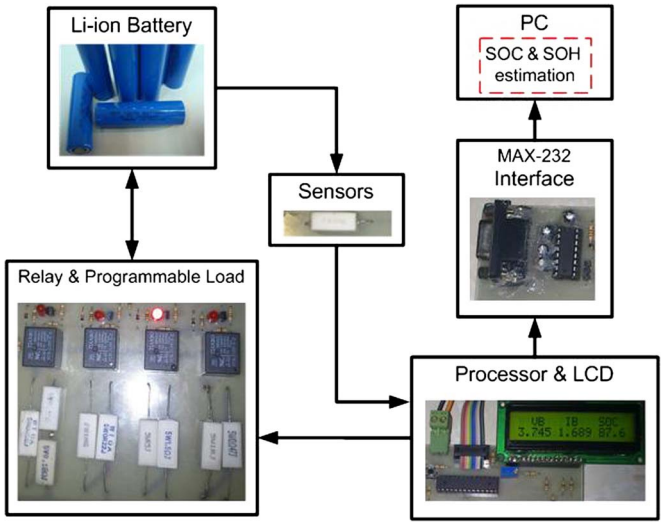

Fig. 2. Schematic of the test setup for lithium-ion battery.

Therefore, from (32), it follows that $\dot{\bar{V}}(\epsilon) \leq 0$. It should be noted that $N = -(A^T P + PA)$ is positive definite.

VI. Experimental Verifications

A. Test Setup

To identify and validate the battery model and verify the proposed SoC and SoH estimation methods, a test system was designed. The battery studied in this test was a lithium-ion battery, which is widely used in laptop computers and has a nominal capacity of 2400 mAh. The nominal, maximum, and cutoff voltages of the battery under study are 3.6, 4.1, and 3 V, respectively. The test system includes a programmable resistive load consisting of a few resistances in parallel and series to control the discharge current of the battery by adding or removing the resistances, a 1-Ω resistance as the current sensor (the voltage drops across this resistor indicate the battery current), an AVR microcontroller to control the load and to measure the current and voltage signals, an LCD for displaying purposes, and a MAX-232 interface for transferring measured data to a PC. Two ADC channels of the microcontroller with 10-b digital output were assigned for the current and voltage signal measurement in a sampling rate of 20 Hz. The test setup is depicted in Fig. 2.

To obtain a discharge profile for the battery, the programmable resistive load is applied. By programming the load, an arbitrary current profile can be generated. These characteristics of the battery can be used for identifying the battery model and evaluating the proposed methods.

B. Model Validation

Based on the model identification scheme proposed by Spagnol *et al.* [35] and from (4) and (7), it follows that

$$V_B = V_{oc} - R_0 I_B - G_m(s)I_B \tag{41}$$

where

$$G_m(s) = \frac{R_s}{1 + sR_sC_s} + \frac{R_f}{1 + sR_fC_f}. \tag{42}$$

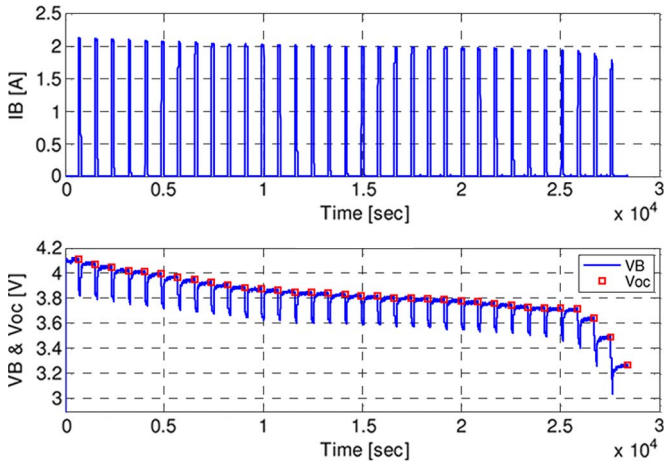

Fig. 3. Discharge current and voltage measured for extracting OCV versus SoC.

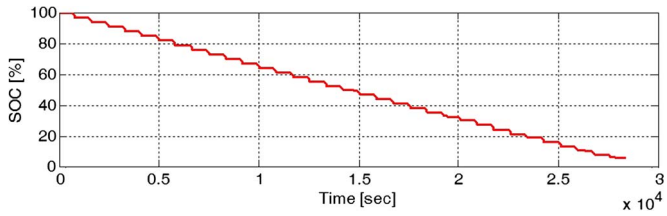

Fig. 4. SoC calculated using the ampere-hour counting method.

In the following, schemes for the identification of V_{oc}, R_0, and $G_m(s)$ parameters are explained.

1) OCV Versus SoC Measurement: The OCV is usually measured as the steady-state open-circuit terminal voltage at different SoCs. However, it takes around a couple of hours to attain steady-state condition. In practice, a shorter idle time, around a quarter of an hour, is enough. In order to extract the OCV versus SoC, a discharge test is run, in which the battery is connected to the programmable resistive load with a resistance of 1.84 Ω and discharged from a fully charge condition by a 0.93-C rate. The discharge and idle times were 120 and 720 s, respectively. The test repeated until the terminal voltage reduced to the cutoff voltage of 3 V. The measured current and voltage during the discharge test are shown in Fig. 3. The squares represent the values of OCV. From the discharge current, the SoC of the battery can be calculated using the ampere-hour counting method. The calculated SoC has been shown in Fig. 4. Moreover, the profile of OCV versus SoC is extracted as shown Fig. 5.

2) Parameter Estimation and Model Validation: To estimate the parameters of the model shown in Fig. 1, we use the discharge test data and (42) in discrete form.

1) C_b: The whole-charge capacitor C_b, neglecting the temperature and cycle dependences, is given by $C_b = 3600 \times (\text{Nominal Capacity})_{\text{Ah}}$. Therefore, it is determined to be 8640 F.
2) R_{sd}: This resistor is estimated so that the SoC obtained from (6) will be consistent with the SoC calculated using the ampere-hour counting method. Therefore, the value of 100 Ω has been obtained for this resistor.
3) R_0: As proposed in [35], to calculate the internal resistance, the ratio of the voltage variation to the current jump

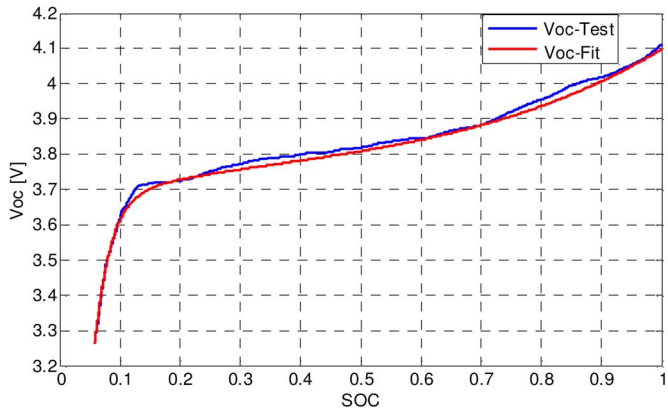

Fig. 5. Measured OCV versus SoC.

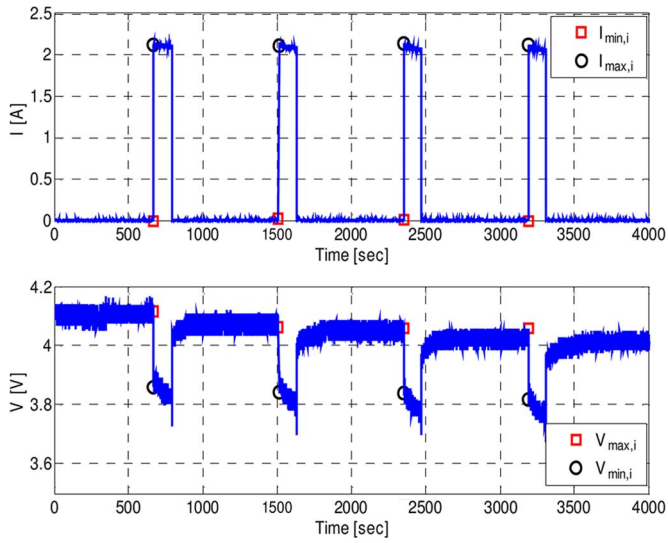

Fig. 6. Current and voltage profiles used for R_0 identification.

is used. The value of R_0 at the ith point of the current jump can be given by

$$R_{0,i} = \frac{v_{\max,i} - v_{\min,i}}{i_{\max,i} - i_{\min,i}} \tag{43}$$

where $v_{\max,i}$, $v_{\min,i}$, $i_{\max,i}$, and $i_{\min,i}$ are shown in Fig. 6. The mean value of $R_{0,i}$ at some points of the current jump, i.e., $R_0 = \Sigma_1^n R_{0,i}/n$, gives the best approximate of R_0.

4) RC networks: For estimating the parameters of the RC networks in the electrical model, (41) is rewritten as follows:

$$V_{oc} - V_B - R_0 I_B = G_m I_B \equiv V_{eq}. \tag{44}$$

Assuming $dI_B/dt \approx 0$ over each sampling period, (44) is discretized as follows:

$$\begin{aligned} V_{eq}[k] &= \left(\frac{R_f(1 - e^{-T_s/T_{pf}})z^{-1}}{1 - e^{-T_s/T_{pf}} z^{-1}} \right. \\ &\quad \left. + \frac{R_s(1 - e^{-T_s/T_{ps}})z^{-1}}{1 - e^{-T_s/T_{ps}} z^{-1}} \right) I_B[k] \\ &= \left(\frac{z^{-1}(b_1 + b_2 z^{-1})}{1 + a_1 z^{-1} + a_2 z^{-2}} \right) I_B[k] \end{aligned} \tag{45}$$

TABLE I
IDENTIFIED RC-NETWORK PARAMETERS

R_0	$88m\Omega$
R_f	$2.8\ m\Omega$
R_s	$41.2\ m\Omega$
C_f	37 F
C_s	1376 F

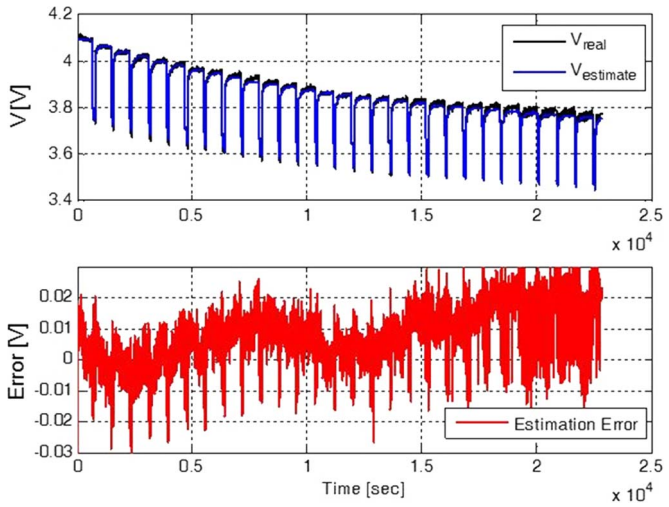

Fig. 7. Measured output voltage versus the model output.

in which T_S is the sampling period and T_{ps} and T_{pf} represent the time constants for the RC subnetworks. Thus, a_1, a_2, b_1, and b_2 are estimated using the dynamic ARMAX model, in which the parameters of the RC networks are obtained. The results of the parameter estimation procedure are given in Table I. With the estimated parameters, the measured and modeled outputs have been compared in Fig. 7. It can be seen that the maximum modeling error is at most 30 mV. For further validation, another discharge test has been applied to the battery. In this case, the discharge and rest intervals are 100 and 700 s, respectively. In Fig. 8, the modeled voltage against the measured one is shown. It is right to conclude that there is a good match between the true voltage and the estimated one with less than 30-mV error.

C. Experimental Verification of Estimators

1) SoC Estimation: Based on the identified parameters of the battery model, the proposed observer is designed. The closed-loop pole set of the observable subsystem is chosen to be $[-0.000116 \quad -0.3 \quad -3]$, which yields to the observer gain $[0.000121 \quad 3.783 \quad -3.661]$. Furthermore, $\mu = 0.5$, $\gamma(t) = 0.005e^{-0.001t}$, and $Q_0 = \mathrm{diag}([0.0001 \quad 0.1 \quad 0.1])$. The discharge current profile of the battery can be seen in Fig. 9. The battery current decreases during discharge, while a constant resistive load was drawing the current.

In Fig. 10, the measured terminal voltage is shown and compared to the estimated terminal voltage by the observer. From this figure, it is clear that the proposed observer demonstrates desirable performance in estimating the terminal voltage. Despite the sudden jumps caused by the current jump, the

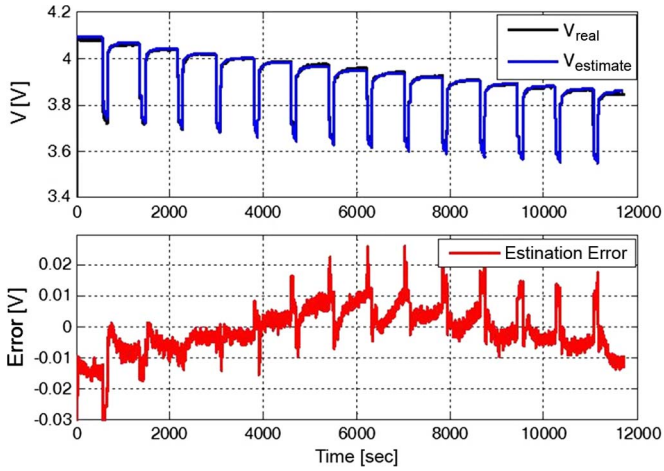

Fig. 8. Comparison of the model-estimated voltage to the measured voltage based on the new current profile.

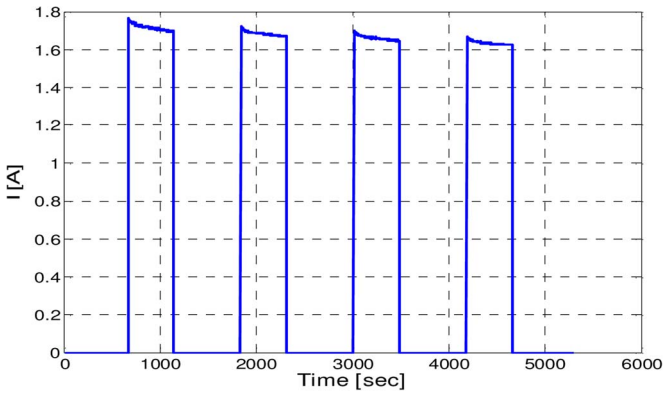

Fig. 9. Discharge current profile of the battery.

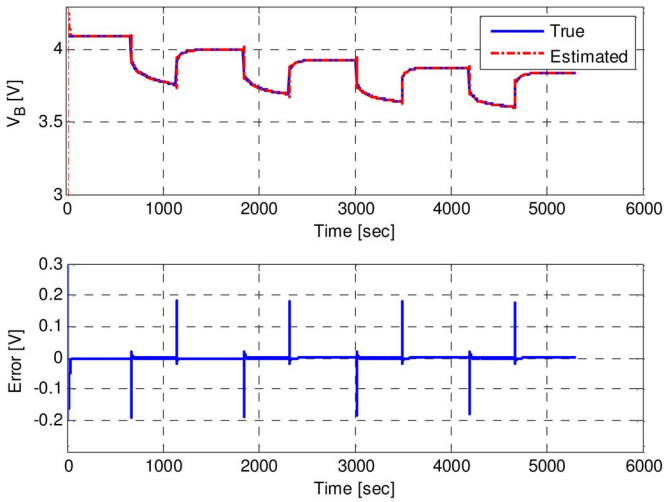

Fig. 10. Estimated terminal voltage compared to the measured profile.

estimation error tends to zero quickly. The amplitude of these jumps depends on the assigned poles of the observer.

The SoC estimation result is given in Fig. 11. It shows that the estimation error is less than 1.2%, when compared to the SoC calculated from the calibrated ampere-hour counting method. The results verify the effectiveness of the proposed scheme for SoC estimation.

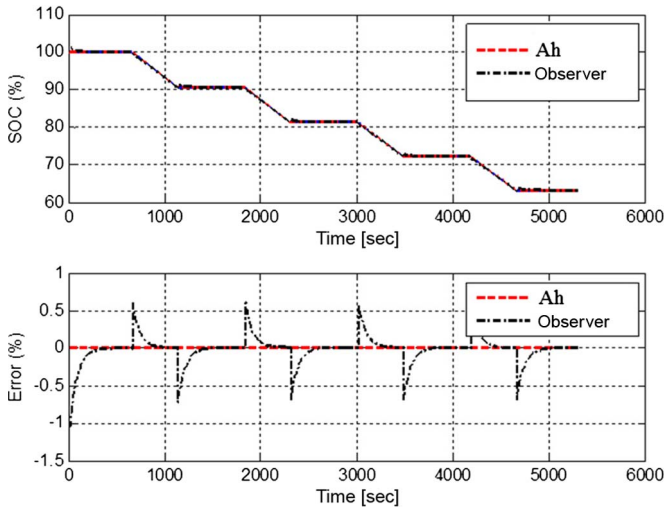

Fig. 11. Estimated SoC compared to the measured profile by precise and calibrated ampere-hour counting.

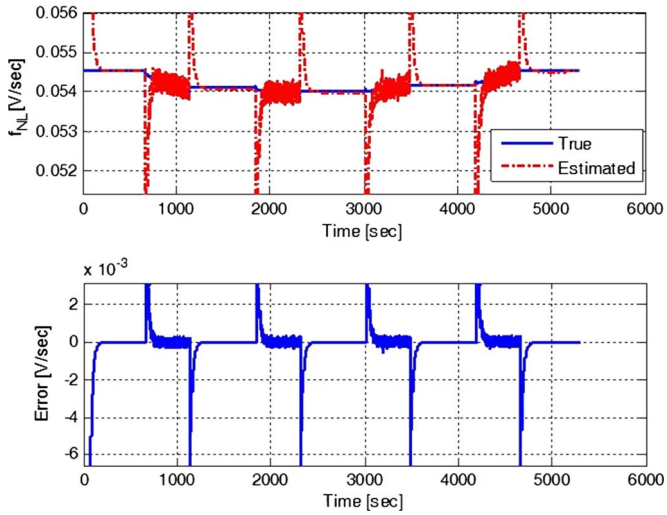

Fig. 12. Estimation of the nonlinear part of the battery model.

2) Estimation of Nonlinearities: The nonlinear term Φ in the lithium-ion battery model is estimated directly based on (30) and compared to the measured profile. The measured profile is obtained by subtracting the output of the linear battery model, i.e., (8) without the additive nonlinear term, from the measured terminal voltage. From Fig. 12, it can be seen that the estimated nonlinear term converges to the measured profile.

3) SoH Estimation: The SoH of the battery is determined based on (33). All the experiments have been performed at room temperature. The initial series resistance of the battery was $R_{0,\text{new}} = 0.088\ \Omega$. Therefore, the EoF resistance is $R_{0,EoF} = 0.1408$. Moreover, the series resistance at the beginning of the experiment was $R_0 = 0.0972\ \Omega$, and thus, the SoH of the test bench battery was determined to be 82.6%.

In order to verify the adaptive scheme for SoH estimation, it was assumed that the series resistance was unknown. The adaptation gain was chosen to be 20. The results of R_0 and SoH estimation using the proposed adaptive method have been shown in Figs. 13–15. In Fig. 13, the adaptive model output (terminal voltage) tracks the measure value, and the estimation

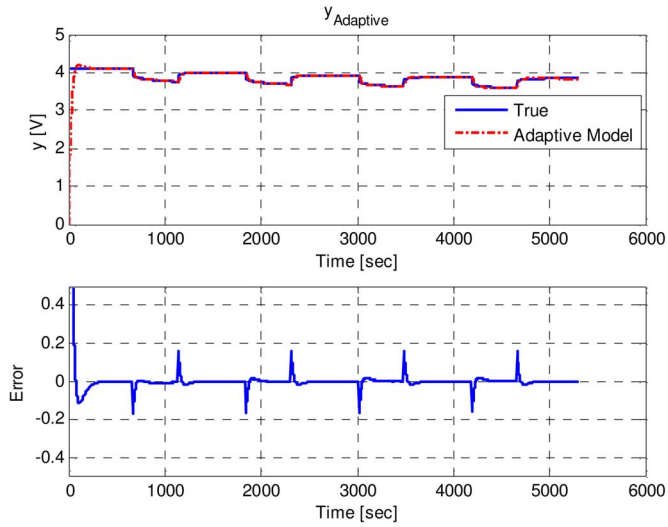

Fig. 13. Adaptive model output compared to the measured terminal voltage.

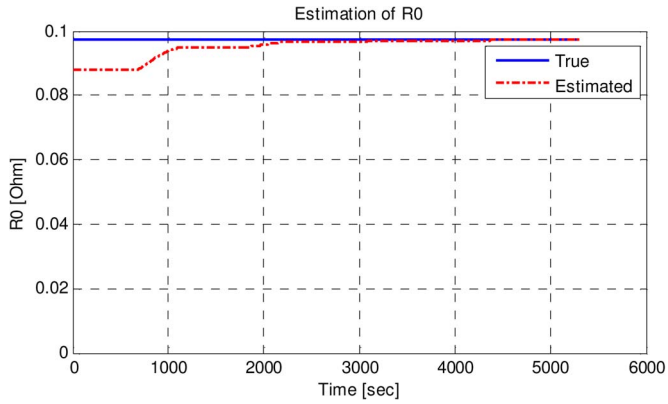

Fig. 14. Estimated series resistance compared to the measured value.

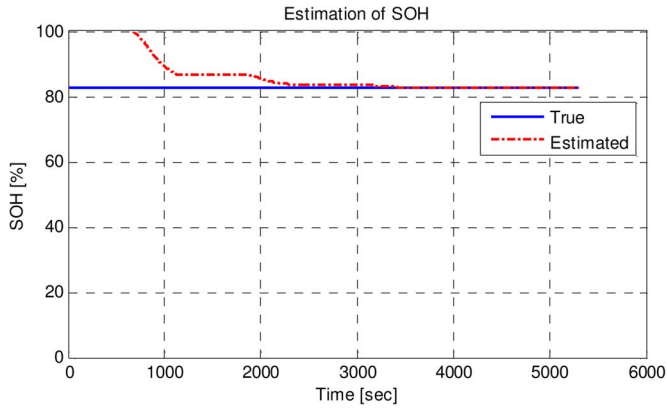

Fig. 15. Estimated SoH compared to the measured value.

error tends to zero. Furthermore, Figs. 14 and 15 verify that the estimated series resistance and SoH converge to their measured values based on offline verifications.

4) Updating Model Resistance Variations With Temperature: In order to consider the thermal effect on model resistances, the battery parameters are updated every 1000 s to adapt to the thermal variations. The flowchart of the proposed updating scheme is shown in Fig. 16. The estimated model resistances based on this scheme are shown in Fig. 17. Moreover, because

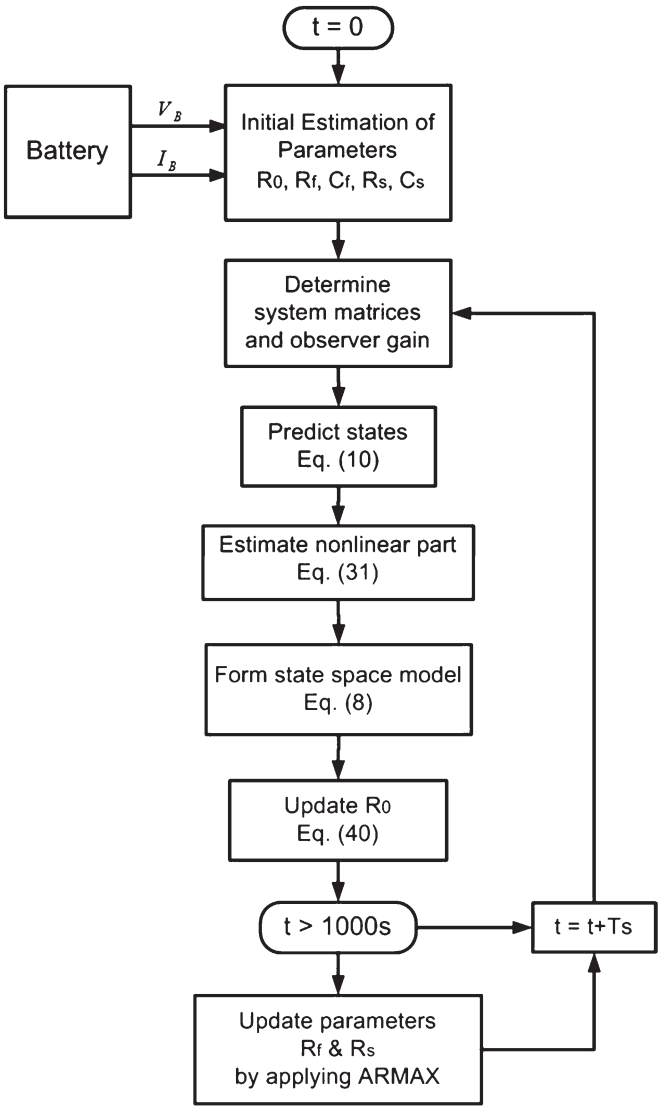

Fig. 16. Updating model resistances based on ARMAX model.

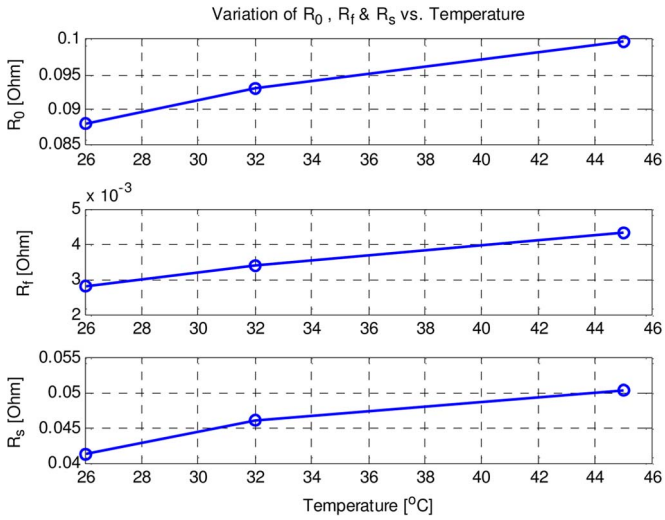

Fig. 17. Updated model resistance values versus temperature.

of using a SMO and the estimation of the nonlinear term, which represents the nonlinear dynamics and uncertainties, the proposed SoC observer is inherently robust to the temperature variations. However, the state of health can be updated based on the modified adaptation of R_0.

VII. Conclusion

Based on an inclusive and unobservable model of the lithium-ion battery, a new scheme for the estimation of the battery SoC is presented. The model is decomposed into the observable and unobservable subsystems. An accurate model for the battery has been developed by estimating the nonlinear part of the battery model. For this purpose, the reachability of the sliding motion is investigated. Using this accurate battery model, an adaptive parameter estimator method has been proposed for estimating the series resistance to monitor the battery SoH. The effectiveness of the proposed schemes has been verified experimentally on a lithium-ion battery, which shows the feasibility and eligibility of the proposed methods in providing accurate estimation of the SoC, nonlinear term in the mathematical model, and SoH of the battery.

References

[1] Y. Hu and S. Yurkovich, "Battery state of charge estimation in automotive applications using LPV techniques," in *Proc. Amer. Control Conf.*, Baltimore, MD, USA, 2010, pp. 5043–5049.

[2] O. Caumont, P. Ph. Le Moigne, and C. Lenain, "An optimized state of charge algorithm for lead-acid batteries in electric vehicles," in *Proc. Electric Vehicle Symp.*, Brussels, Belgium, 1998, vol. EVS-15, [CD-ROM].

[3] H. Dai, Z. Sun, and X. Wei, "Online SOC estimation of high-power lithium-ion batteries used on HEV's," in *Proc. IEEE Int. Conf. Veh. Electron. Safety*, 2006, pp. 342–347.

[4] M. Coleman, C. K. Lee, C. Zhu, and W. G. Hurley, "State-of-charge determination from EMF voltage estimation: Using impedance, terminal voltage, and current for lead-acid and lithium-ion batteries," *IEEE Trans. Ind. Electron.*, vol. 54, no. 5, pp. 2550–2557, Oct. 2007.

[5] B. S. Bhangu, P. Bentley, D. A. Stone, and C. M. Bingham, "Nonlinear observers for predicting state-of-charge and state-of-health of lead-acid batteries for hybrid-electric vehicles," *IEEE Trans. Veh. Technol.*, vol. 54, no. 3, pp. 783–794, May 2005.

[6] S. Lee, J. Kim, J. Lee, and B. Cho, "State-of-charge and capacity estimation of lithium-ion battery using a new open circuit voltage versus state-of-charge," *J. Power Sourc.*, vol. 185, no. 2, pp. 1367–1373, Dec. 2008.

[7] D. Di Domenico, G. Fiengo, and A. Stefanopoulou, "Lithium-ion battery state of charge estimation with a Kalman filter based on a electrochemical model," in *Proc. IEEE Int. Conf. CCA*, 2008, pp. 702–707.

[8] G. L. Plett, "Extended Kalman filtering for battery management systems of LiPB-based HEV battery packs, Part 2: Modeling and identification," *J. Power Source*, vol. 134, no. 2, pp. 262–276, Aug. 2004.

[9] G. L. Plett, "Extended Kalman filtering for battery management systems of LiPB-based HEV battery packs, Part 3: State and parameter estimation," *J. Power Source*, vol. 134, no. 2, pp. 277–292, Aug. 2004.

[10] V. Pop, H. J. Bergveld, D. Danilov, and P. H. Notten, *Battery Management Systems, Accurate State-of Charge Indication for Battery-Powered Applications*. New York, NY, USA: Springer-Verlag, 2008.

[11] J. Kim and B. H. Cho, "State-of-charge estimation and state-of-health prediction of a Li-ion degraded battery based on an EKF combined with a per unit system," *IEEE Trans. Veh. Technol.*, vol. 60, no. 9, pp. 4249–4260, Nov. 2011.

[12] J. Kim, S. Lee, and B. H. Cho, "Complementary cooperation algorithm based on DEKF combined with pattern recognition for SOC/capacity estimation and SOH prediction," *IEEE Trans. Power Electron.*, vol. 27, no. 1, pp. 436–451, Jan. 2012.

[13] G. Plett, "Sigma-point Kalman filtering for battery management systems of LIPB-based HEV battery packs: Part 2: Simultaneous state and parameter estimation," *J. Power Source*, vol. 161, no. 2, pp. 1369–1384, Oct. 2006.

[14] R. Xiong, H. He, F. Sun, and K. Zhao, "Evaluation on state of charge estimation of batteries with adaptive extended Kalman filter by experiment approach," *IEEE Trans. Veh. Technol.*, vol. 62, no. 1, pp. 108–117, Jan. 2013.

[15] F. Zhang, G. Liu, L. Fang, and H. Wang, "Estimation of battery state of charge with $H\infty$ observer: Applied to a robot for inspecting power transmission lines," *IEEE Trans. Ind. Electron.*, vol. 59, no. 2, pp. 1086–1095, Feb. 2012.
[16] Y. Li, R. D. Anderson, J. Song, A. M. Phillips, and X. Wang, "A nonlinear adaptive observer approach for state of charge estimation of lithium-ion batteries," in *Proc. Amer. Control Conf.*, San Francisco, CA, USA, 2011, pp. 370–375.
[17] P. Singh, C. Fennie, and D. E. Reisner, "Fuzzy logic modeling of state-of-charge and available capacity of nickel/metal hydride batteries," *J. Power Sourc.*, vol. 136, no. 2, pp. 322–333, Oct. 2004.
[18] C. H. Cal, D. Du, Z. Y. Liu, and H. Zhang, "Artificial neural network in estimation of battery state-of-charge (SOC) with nonconventional input variables selected by correlation analysis," in *Proc. MLC*, Beijing, China, 2002, pp. 1619–1625.
[19] Y.-S. Lee, W.-Y. Wang, and T.-Y. Kuo, "Soft computing for battery state-of-charge (BSOC) estimation in battery string systems," *IEEE Trans. Ind. Electron.*, vol. 55, no. 1, pp. 229–239, Jan. 2008.
[20] M. Charkhgard and M. Farrokhi, "State-of-charge estimation for lithium-ion batteries using neural networks and EKF," *IEEE Trans. Ind. Electron.*, vol. 57, no. 12, pp. 4178–4187, Dec. 2010.
[21] H.-T. Lin, T.-J. Liang, and S.-M. Chen, "Estimation of battery state of health using probabilistic neural network," *IEEE Trans. Ind. Inf.*, vol. 9, no. 2, pp. 679–685, May 2013.
[22] A. R. P. Robat and F. R. Salmasi, "State of charge estimation for batteries in HEV using locally linear model tree (LOLIMOT)," in *Proc. ICEMS*, Seoul, South Korea, 2007, pp. 2041–2045.
[23] N. Watrin, B. Blunier, and A. Miraoui, "Review of adaptive systems for lithium batteries state-of-charge and state-of-health estimation," in *Proc. IEEE Trans. Electrificat. Conf.*, 2012, pp. 1–6.
[24] M. Shahriari and M. Farrokhi, "Online state-of-health estimation of VRLA batteries using state of charge," *IEEE Trans. Ind. Electron.*, vol. 60, no. 1, pp. 191–202, Jan. 2013.
[25] A. H. Ranjbar, A. Banaei, A. Khoobroo, and B. Fahimi, "Online estimation of state of charge in Li-ion batteries using impulse response concept," *IEEE Trans. Smart Grid*, vol. 3, no. 1, pp. 360–367, Mar. 2012.
[26] F. Zhang, G. Liu, and L. Fang, "A battery state of charge estimation method using sliding mode observer," in *Proc. 7th World Congr. Intell. Control Autom.*, Jun. 2008, pp. 989–994.
[27] I.-S. Kim, "The novel state of charge estimation method for lithium battery using sliding mode observer," *J. Power Sourc.*, vol. 163, no. 1, pp. 584–590, Dec. 2006.
[28] I.-S. Kim, "A technique for estimating the state of health of lithium batteries through a dual-sliding-mode observer," *IEEE Trans. Power. Electron.*, vol. 25, no. 4, pp. 1013–1022, Apr. 2010.
[29] M. Einhorn, F. Valerio Conte, C. Kral, and J. Fleig, "A method for online capacity estimation of lithium-ion battery cells using the state of charge and the transferred charge," *IEEE Trans. Ind. Appl.*, vol. 48, no. 2, pp. 736–741, Mar./Apr. 2012.
[30] M. Chen and G. A. Rincon-Mora, "Accurate electrical battery model capable of predicting runtime and I-V performance," *IEEE Trans. Energy Convers.*, vol. 21, no. 2, pp. 504–511, Jun. 2006.
[31] C. Edwards, S. K. Spurgeon, C. P. Tan, and N. Patel, *Sliding-Mode Observers*. Berlin, Germany: Springer-Verlag, 2007.
[32] X. G. Yan and C. Edwards, "Adaptive sliding-mode-observer-based fault reconstruction for nonlinear systems with parametric uncertainties," *IEEE Trans. Ind. Electron.*, vol. 55, no. 11, pp. 4029–4036, Nov. 2008.
[33] M. Cugnet, J. Sabatier, S. Laruelle, S. Grugeon, B. Sahut, A. Oustaloup, and J. Tarascon, "On lead-acid battery resistance and cranking-capability estimation," *IEEE Trans. Ind. Electron.*, vol. 57, no. 3, pp. 909–917, Mar. 2010.
[34] D. Haifeng, W. Xuezhe, and S. Zechang, "A New SOH prediction concept for the power lithium-ion battery used on HEVs," in *Proc. IEEE VPPC*, 2009, pp. 1649–1653.
[35] P. Spagnol, S. Rossi, and S. M. Savaresi, "Kalman filter SOC estimation for Li-ion batteries," in *Proc. IEEE Int. CCA*, 2011, pp. 587–592.

Mehdi Gholizadeh received the B.S. and M.S. degrees in control engineering from the University of Tehran, Tehran, Iran, in 2009 and 2012, respectively.

His research interests include battery management systems, battery charging, estimation techniques, robust adaptive observers, and self-oscillating adaptive systems.

Farzad R. Salmasi (S'99–M'02–SM'09) received the B.S. degree in electrical engineering from the Sharif University of Technology, Tehran, Iran, in 1994, the M.Sc. degree in electrical engineering from the Amirkabir University of Technology, Tehran, in 1997, and the Ph.D. degree in electrical engineering from Texas A&M University, College Station, TX, USA, in 2002.

From 1999 to 2002, he worked as a Research Assistant for the Advanced Motor Drives and Hybrid Vehicles Laboratory, Department of Electrical engineering, Texas A&M University. From 2002 to 2004, he was with the Electro Standards Laboratories, Cranston, RI, USA, as a Research Scientist. In September 2004, he joined the School of Electrical and Computer Engineering, Faculty of Engineering, University of Tehran. He is currently the Head of the Control Engineering Department. His main research areas include the design and control of advanced motor drives, power electronic systems, hybrid electric vehicles, networked control systems, and smart grids.

Dr. Salmasi is a technical committee member of the International Association of Science and Technology for Development on power and energy systems.